

## Distinctive Fluctuations in a Confined Geometry

M. Degawa,<sup>1,\*</sup> T. J. Stasevich,<sup>1</sup> W. G. Cullen,<sup>1</sup> Alberto Pimpinelli,<sup>1,2,†</sup> T. L. Einstein,<sup>1,‡</sup> and E. D. Williams<sup>1,§</sup>

<sup>1</sup>Department of Physics, University of Maryland, College Park, Maryland 20742-4111 USA

<sup>2</sup>LASMEA, UMR 6602 CNRS, Université Blaise Pascal - Clermont 2, F-63177 Aubière, France

(Received 2 February 2006; revised manuscript received 30 May 2006; published 21 August 2006)

Spurred by recent theoretical predictions [Phys. Rev. E **69**, 035102(R) (2004); Surf. Sci. Lett. **598**, L355 (2005)], we find experimentally using STM line scans that the fluctuations of the step bounding a facet exhibit scaling properties distinct from those of isolated steps or steps on vicinal surfaces. The correlation functions go as  $t^{0.15 \pm 0.03}$  decidedly different from the  $t^{0.26 \pm 0.02}$  behavior for fluctuations of isolated steps. From the exponents, we categorize the universality, confirming the prediction that the nonlinear term of the Kardar-Parisi-Zhang equation, long known to play a central role in nonequilibrium phenomena, can also arise from the curvature or potential-asymmetry contribution to the step free energy.

DOI: 10.1103/PhysRevLett.97.080601

PACS numbers: 05.40.-a, 65.80.+n, 68.37.Ef, 81.07.-b

Technological demands on the fabrication and properties of nanostructures [1] provide renewed motivation for understanding the properties that control morphology changes on the nanoscale. In the past decade, the step continuum model has allowed several successful quantitative correlations of direct observations of step fluctuations with kinetic and thermodynamic descriptions of nanoscale structural evolution [2–6]. For complex structures where mass transport is limited by geometry, the fundamental question of how fluctuations behave in a constrained environment becomes experimentally accessible. For an isolated step on a flat fcc(111) metal surface, experimental results typically show that the principal mass transport mechanism is step-edge diffusion (SED), with time correlations  $t^{1/4}$  at low temperature  $T$  [3,5,6], and crosses over to other behavior with increasing  $T$  [7]. However, for smaller structures, issues of finite volume (shape effects and volume conservation) become non-negligible [8,9]. Although the step can still be viewed as a 1D interface obeying a Langevin-type equation of motion, not only local deformation but global effects must be considered when calculating the step chemical potential. These considerations alter the equation of motion, including the noise term, resulting in different universality classes of dynamic scaling [10].

Finite-volume effects on nanocrystallites with a Gruber-Mullins-Pokrovsky-Talapov surface free energy density [11] have been found to produce metastable states with different crystal shapes [12] for a given crystal-substrate interface boundary condition [9,13]. All shapes have a facet smoothly connected to a vicinal region, which obeys an  $x^{3/2}$  shape power law in equilibrium [14]. Once a crystallite attains a stable state, the step that serves as the interface between the facet and the vicinal region [see Fig. 1(b)] fluctuates around its stable position, which is determined by the asymmetric potential established by step-step interactions and the “reservoir” chemical potential of the crystallite. When step interactions are solely entropic, recent theoretical work [15], within a terrace-step-kink (TSK) model with volume conservation, estab-

lishes rigorously that the static scaling of the facet-edge fluctuations have a roughness exponent  $\alpha = 1/3$ , different from  $\alpha = 1/2$  of a random walk. From heuristic and scaling perspectives, some of us [16] reobtained  $\alpha = 1/3$  for facet-edge fluctuations in a way that suggests this result holds even when elastic effects supplement the entropic repulsion between steps. The effect of the asymmetric potential can be directly evaluated from the step chemical potential [17,18], and then enters the equation of motion as a nonlinear term of the form  $(\nabla x)^2$ , characteristic of the Kardar-Parisi-Zhang (KPZ) equation [19], if the fluctuations are small compared to the interstep spacing. The KPZ term affects the noise term and restricts the amplitude of fluctuation, which leads to different scaling properties of the noise. Extensions to dynamic scaling yield a growth exponent  $\beta = 1/5$  or  $\beta = 1/11$ , depending on the limiting kinetics, attachment-detachment (AD) or SED, respectively [16]. General considerations of the various universality classes [20,21] that can arise for different types of spatial confinement for the two cases of limiting kinetics are summarized in Table I.

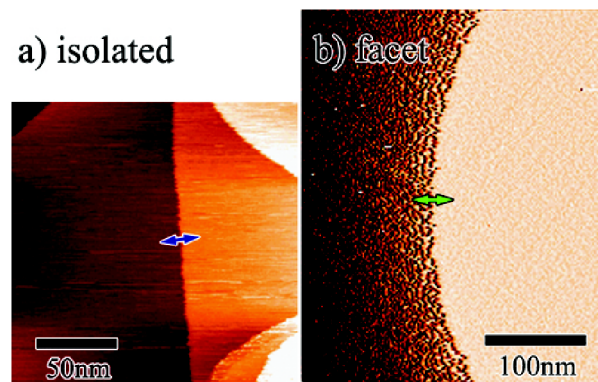


FIG. 1 (color online). An STM image of (a) an isolated step on a crystallite facet (room temperature) and (b) a crystal facet edge (350 K). The small superimposed double arrows indicate the tip path that leads to line-scan images as in Fig. 2.

TABLE I. Summary of the dynamical scaling universality classes for crystallite steps. The geometries included are: Free = an isolated step or island edge, Sym-cfn = steps symmetrically confined by the nearby steps as in a step bunch, and Asy-cfn = steps confined by an asymmetric potential, especially a facet edge. The KPZ class is included for comparison. In the underlying Langevin equation (cf. Ref. [20]),  $l$  or  $n$  indicates whether the equation is linear or nonlinear (has a KPZ term).  $C$  or  $N$  indicates whether the deterministic part and the noise are conservative or nonconservative;  $M$  denotes mixed, with the former conservative but the noise not. The superscript (2 or 4) indicates the power of  $\nabla$  in the linear conservative term, while the subscript gives the dimensionality of the independent variable.

Geom.	AD	$\alpha$	$2\beta$	$z$	SED	$\alpha$	$2\beta$	$z$
Free	$IM_1^2(\text{EW})$	$\frac{1}{2}$	$\frac{1}{2}$	2	$IC_1^4$	$\frac{1}{2}$	$\frac{1}{4}$	4
Sym-cfn	$IM_2^2$	0	0	2	$IC_2^4$	0	0	4
Asy-cfn	KYP [22]	$\frac{1}{3}$	$\frac{2}{5}$	$\frac{5}{3}$	$nC_1^4$	$\frac{1}{3}$	$\frac{2}{11}$	$\frac{11}{3}$
KPZ	$nN_1^2$	$\frac{1}{2}$	$\frac{2}{3}$	$\frac{3}{2}$	$nM_2^4$	$\frac{2}{3}$	$\frac{2}{5}$	$\frac{10}{3}$

Here we report the first experimental observations of the novel scaling predicted for facet-edge fluctuations on crystallites. Our crystallites were formed by depositing a 20–30 nm Pb film at room  $T$  on a Ru(0001) substrate in UHV [23], and subsequently dewetting at 620 K. The liquid Pb droplets solidified upon slow cooling and were left to equilibrate to a stable state at the  $T$  of the experiment [23,24]. The crystallites are observed with a variable-temperature scanning tunneling microscope (VT-STM) after equilibration. Figure 1 depicts a STM image of (a) an isolated step (room temperature) and (b) facet edge (350 K). A crystallite in a stable state as shown in Fig. 1(b) has a flat, close-to-circular (111) facet and a smoothly-connecting vicinal region.

By repeatedly scanning perpendicularly to a single position along the facet-edge or step (cf. Figure 1), we obtain a line-scan STM image [3]  $x(t)$ , as shown in Fig. 2 for

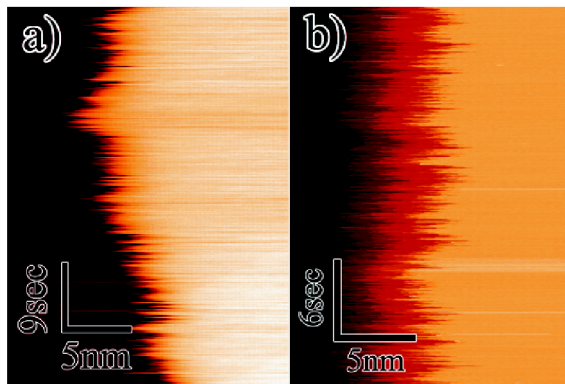


FIG. 2 (color online). Segment of a line-scan image of (a) an isolated step (step from screw dislocation) and (b) a facet edge at 350 K, showing also the correlated fluctuations of the neighboring steps. The time interval between lines is 0.02 s, and 2000 lines are measured per image.

(a) an isolated step (step from a screw dislocation) and (b) a facet edge, both at 350 K. Digitized step positions  $x(t)$  extracted from these “pseudoimages” are used for statistical analysis. To evaluate the growth exponent  $\beta$ , we calculate the early behavior of the time correlation function  $G(t)$

$$G(t) = \langle [x(t + t_0) - x(t_0)]^2 \rangle_{t_0} \sim t^{2\beta}. \quad (1)$$

To evaluate the roughness exponent  $\alpha$ , we calculate the saturation value of the width  $w$  of the fluctuating step:

$$w^2 = \langle [x(t) - \bar{x}]^2 \rangle \sim L^{2\alpha}, \quad (2)$$

where  $L$  is the system size.

In Fig. 3 we show the time correlation function  $G(t)$  measured for (a) facet edges and (b) isolated-step edges. Squares, circles, and triangles correspond to measurements at 300 K, 350 K, and 400 K, respectively. Each curve represents the average over the correlation functions for 10–30 measurements of  $x(t)$ . The slope of the curves on the log-log plot yields the exponent  $2\beta$ . The values for the individual curves are listed in the figure caption. As expected, the exponents show no systematic dependence on

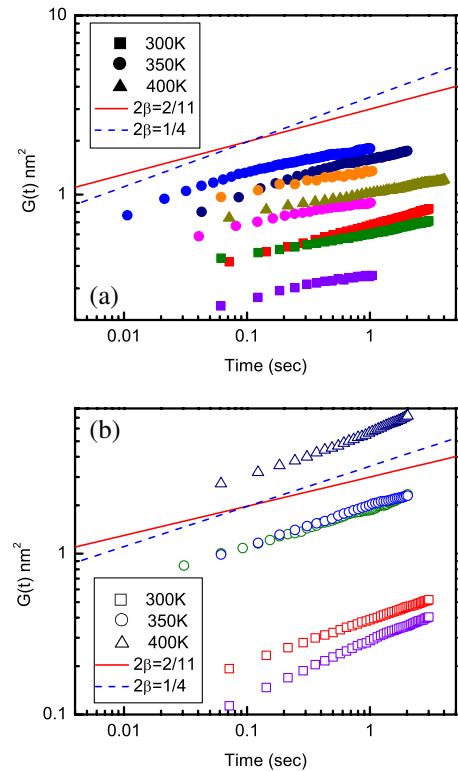


FIG. 3 (color online). Log-log plot of  $G(t)$  [Eq. (1)] of (a) facet edges and (b) isolated steps with facet radii from 60 to 190 nm. The symbols represent 300 K (squares), 350 K (circles), and 400 K (triangles). For guidance, solid and dashed lines show slopes  $2/11$  and  $1/4$ , respectively. Individual fits to each of the data sets yield slopes of (a) facet edges: 300 K ( $0.18 \pm 0.01$ ,  $0.13 \pm 0.06$ ,  $0.13 \pm 0.02$ ), 350 K ( $0.17 \pm 0.04$ ,  $0.17 \pm 0.04$ ,  $0.12 \pm 0.03$ ,  $0.11 \pm 0.05$ ); 400 K ( $0.12 \pm 0.12$ ), and (b) isolated steps: 300 K ( $0.32 \pm 0.03$ ,  $0.26 \pm 0.008$ ), 350 K ( $0.24 \pm 0.03$ ,  $0.24 \pm 0.04$ ), 400 K ( $0.30 \pm 0.04$ ).

$T$ ; from all data sets, the  $\sigma^{-2}$ -weighted average exponent is  $2\beta = 0.149 \pm 0.032$  for facet edges and  $2\beta = 0.262 \pm 0.021$  for isolated steps. With over 99.9% significance (Student's  $t$  test) these values come from different parent populations. Each of the two results is within 1 standard deviation,  $\sigma$ , of the respective predicted values.

To determine the roughness exponent  $\alpha$ , system-size dependence must be evaluated. For the confined steps [Fig. 3(a)], we assume  $L \sim R$  (the facet radius), so we expect  $w^2 \sim R^{2\alpha}$ . (For the unconfined steps, the system size is larger than the limitations imposed by the finite measurement time, as discussed previously [5].) Figure 3(a) reveals the effects of the facet size, since the three upper sets of data at 350 K were taken on larger crystallites (radius  $>100$  nm). More quantitatively, in Fig. 4 we plot the characteristic length  $w^2 \tilde{\beta}/k_B T$  vs facet radius at 300 K and 350 K, using  $\tilde{\beta} = 0.339$  eV/nm and  $0.327$  eV/nm [25], respectively. Fits to the data yield exponents within the predicted range of  $\alpha = 1/3$  (solid) to  $\alpha = 1/2$  (dash). Although there are insufficient data to distinguish between these two values [26], the results clearly show the effect of  $R$  on the fluctuations, providing further evidence that effects of crystal confinement govern the behavior of  $G(t)$ .

The facet-edge fluctuations manifest a different universality class of dynamic scaling from that of an isolated step on a surface. Unlike previous predictions for step exponents [2,3,7,27], this difference is not attributed to the type of kinetics. Instead, the effect is predicted to result from the coupling of the step chemical potential to the fluctuations. For facet-edge fluctuations the step confinement is due to an increase in local step chemical potential  $\mu(x)$  when the step is displaced from equilibrium. The functional behavior of  $\mu(x)$  results from a competition between the step-repulsions from the vicinal region and the 2d pressure of the adatom density on the facet, which in turn is defined by the constraints governing the crystallite shape [9,12]. For a step symmetrically confined on a vicinal surface, the confinement corresponds to a force that is quadratic in dis-

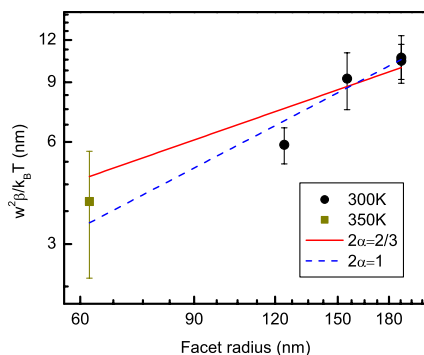


FIG. 4 (color online). Product of squared saturation width and reduced stiffness as a function of facet radius (facet edge only). Circles and squares are room temperature and 350 K, respectively. Solid and dashed lines are a fit to the 350 K data with  $\alpha = 1/3$  and  $\alpha = 1/2$ , respectively.

placement [28]. However, for the facet-edge step, the asymmetry in the  $\mu(x)$  corresponds to an asymmetric confining force that includes a cubic term in displacement [29]. These conditions of the confined facet-edge step lead to nonlinear terms in the equation of motion, as discussed above.

To elucidate the physics of asymmetric confinement in a conserved-volume system with SED-limited kinetics, we have performed standard Monte Carlo (MC) simulations of a simple TSK model on a square lattice in which a single active step is placed a distance  $d$  lattice constants from a second fixed straight step, both steps have projected length  $L_y$  [18]. For convenience we set  $k_B T$  at the energy  $\epsilon$  of a unit length of step and assume only entropic interactions between the two steps. The active step evolves by Kawasaki dynamics, with trial moves by “atoms” at the step to neighboring sites along the step. Most of our runs were done with  $L_y = 100$ , with  $\sim 10^8$  MC steps per site; consistent with the high value of  $z$  for SED dynamics, runs with  $L_y = 200$  are hard to converge. As shown in Fig. 5, after random-walk ( $\beta = 1/4$ ) evolution at the very outset (first few points),  $G(t)$  quickly crosses over to isolated-step ( $\beta = 1/8$ ) behavior. For  $d = 4$ , once the step meanders enough to be affected by the fixed step,  $G(t)$  crosses over to asymmetric conserved-volume confinement ( $\beta = 1/11$ ), then eventually begins to cross over to flat late-time behavior of symmetrically confined steps. For  $d = 2$ , confinement is so great that  $G(t)$  progresses quickly from initial- to late-time evolution, with no clear intermediate regime. For  $d = 500$ , much larger than the mean squared width of the step  $w^2$ , the fixed step never significantly influences the active one. Similar behavior is already seen for  $d = 6$ . That the experimental value of  $2\beta = 0.15 \pm 0.03$  is somewhat below  $2/11$  weakly suggests (one-sigma level) that some physical effect may be acting to reduce the growth exponent. The possibility of extreme damping of fluctuations due to small step spacings, as for

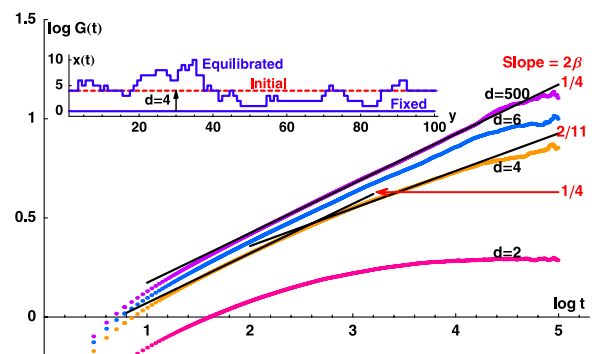


FIG. 5 (color online). Log-log plot of  $G(t)$  from MC simulation using the toy model described in the text and sketched in the inset, for spacings  $d$  between the active and the single fixed step ranging from 2 to 500. The solid straight lines have the two predicted slopes  $2/11$  and  $1/4$ . We see that  $\beta$  increases smoothly with increasing  $d$ , i.e., with decreasing asymmetric entropic interaction.

$d = 2$  in Fig. 5, is unlikely since our Pb measurements correspond to  $d/w$  values  $\sim 5$ – $10$ , well above the strong-confinement regime. Thorough analysis of a more detailed model would be needed for quantification.

Study of spatial correlations (in a log-log plot of  $\langle [x(y + y_0) - x(y_0)]^2 \rangle_{y_0} \sim y^{2\alpha}$ , not shown) likewise suggests that  $\alpha$  increases from  $1/3$  at  $d = 4$  to  $1/2$  at  $d = 500$ , albeit with linear scaling over less than a decade in  $y$  [18].

We have experimentally, for the first time, observed evidence for a nonlinear term in equilibrium fluctuations. The result agrees with predictions for the case of geometrically confined fluctuations. Our measured value is significantly smaller than the unconfined exponent of  $\beta = 1/8$ , and is within  $1\sigma$  of the predicted value of  $\beta = 1/11$  for a universality class of dynamical scaling with  $\alpha = 1/3$  and  $z = 11/3$ . Although KPZ behavior has been earlier linked to the behavior of facet edges [30], this is the first time to our knowledge that a KPZ-type equation of motion has accounted for equilibrium fluctuations. Change in the fluctuations and equation of motion for steps in a perturbed environment [31] may introduce new opportunities in controlling the fabrication of nanostructures, or in new aspects of their dynamic properties.

Work at University of Maryland has been supported by the UMD-NSF MRSEC under Grant No. DMR 05-20471 with initial support from DOE; visits by A. P. supported by a CNRS Travel Grant. The shared experimental facilities of the MRSEC were used in the experimental work.

\*Email address: mdegawa44@hotmail.com

†Email address: alpimpin@univ-bpclermont.fr

‡Email address: einstein@umd.edu

§Email address: edw@umd.edu

- [1] I. Lyubnitsky *et al.*, J. Appl. Phys. **94**, 7926 (2003); Z. Gai *et al.*, Phys. Rev. Lett. **89**, 235502 (2002); J. Tersoff, C. Teichert, and M. G. Lagally, Phys. Rev. Lett. **76**, 1675 (1996); C. Teichert, M. G. Lagally, L. J. Peticolas, J. C. Bean, and J. Tersoff, Phys. Rev. B **53**, 16334 (1996).
- [2] H. C. Jeong and E. D. Williams, Surf. Sci. Rep. **34**, 171 (1999).
- [3] M. Giesen, Prog. Surf. Sci. **68**, 1 (2001).
- [4] I. Lyubnitsky, D. B. Dougherty, T. L. Einstein, and E. D. Williams, Phys. Rev. B **66**, 085327 (2002).
- [5] O. Bondarchuk *et al.*, Phys. Rev. B **71**, 045426 (2005).
- [6] L. Kuipers, M. S. Hoogeman, J. W. M. Frenken, and H. van Beijeren, Phys. Rev. B **52**, 11387 (1995); S. Speller *et al.*, Surf. Sci. **333**, 1056 (1995).
- [7] T. Ihle, C. Misbah, and O. Pierre-Louis, Phys. Rev. B **58**, 2289 (1998); S. V. Khare and T. L. Einstein, Phys. Rev. B **57**, 4782 (1998); M. Ondrejcek, M. Rajappan, W. Swiech, and C. P. Flynn, Phys. Rev. B **73**, 035418 (2006).
- [8] Z. Kuntova, Z. Chvoj, V. Sima, and M. C. Tringides, Phys. Rev. B **71**, 125415 (2005).
- [9] M. Degawa, F. Szalma, and E. D. Williams, Surf. Sci. **583**, 126 (2005).
- [10] H. Gebremariam, Ph.D. thesis, University of Maryland, 2005.
- [11] V. L. Pokrovsky and A. L. Talapov, Phys. Rev. Lett. **42**, 65 (1979).
- [12] M. Uwaha and P. Nozières, in *Morphology and Growth Unit of Crystals*, edited by I. Sunagawa (Terra Scientific Publishing Co., Tokyo, 1989), p. 17.
- [13] W. L. Winterbottom, Acta Metall. Mater. **15**, 303 (1967); P. Müller and R. Kern, Surf. Sci. **457**, 229 (2000).
- [14] M. Wortis, in *Chemistry and Physics of Solid Surfaces VII*, edited by R. Vanselow and R. F. Howe (Springer Verlag, Berlin, 1988), p. 367; P. Nozières, in *Solids Far from Equilibrium*, edited by C. Godrèche (Cambridge University Press, Cambridge, 1991), p. 1; S. Balibar, H. Alles, and A. Y. Parshin, Rev. Mod. Phys. **77**, 317 (2005); A. Pavlovskaya, D. Dobrev, and E. Bauer, Surf. Sci. **326**, 101 (1995); C. Rottman, M. Wortis, J. C. Heyraud, and J.-J. Métois, Phys. Rev. Lett. **52**, 1009 (1984).
- [15] P. L. Ferrari, M. Prähofer, and H. Spohn, Phys. Rev. E **69**, 035102(R) (2004).
- [16] A. Pimpinelli *et al.*, Surf. Sci. Lett. **598**, L355 (2005).
- [17] M. Degawa and E. D. Williams, Surf. Sci. **595**, 87 (2005).
- [18] M. Degawa, Ph.D. thesis, University of Maryland, 2006; Proceedings of the European Conference on Surface Science, Paris, 2006, [Surf. Sci. (to be published)].
- [19] M. Kardar, G. Parisi, and Y. C. Zhang, Phys. Rev. Lett. **56**, 889 (1986).
- [20] A.-L. Barabási and H. E. Stanley, *Fractal Concepts in Surface Growth* (Cambridge University Press, Cambridge, 1995).
- [21] H. G. E. Hentschel and F. Family, Phys. Rev. Lett. **66**, 1982 (1991).
- [22] Y. Kim, S. Y. Yoon, and H. Park, Phys. Rev. E **66**, 040602 (2002) present MC results for a restricted solid-on-solid model, which also includes a somewhat artificial mechanism to limit the fluctuation width. They find  $\beta \approx 2/9$  and  $z \approx 3/2$ .
- [23] K. Arenhold *et al.*, Surf. Sci. **424**, 271 (1999); C. Bombis *et al.*, Surf. Sci. **511**, 83 (2002); M. Nowicki *et al.*, New J. Phys. **4**, 60 (2002).
- [24] K. Thürmer *et al.*, Phys. Rev. Lett. **87**, 186102 (2001); K. Thürmer, J. E. Reutt-Robey, and E. D. Williams, Surf. Sci. **537**, 123 (2003).
- [25] N. Akutsu and Y. Akutsu, J. Phys. Condens. Matter **11**, 6635 (1999); M. Nowicki, C. Bombis, A. Emundts, and H. P. Bonzel, Phys. Rev. B **67**, 075405 (2003).
- [26] Although  $\alpha = 1/2$  gives a better fit, there is insufficient data to draw a definitive conclusion. Direct experimental observation, e.g., of the spatial correlation function on a quenched crystallite, is needed to obtain  $\alpha$  for facet-edge fluctuations.
- [27] E. Le Goff, L. Barbier, and B. Salanon, Surf. Sci. **531**, 337 (2003); M. Ondrejcek, W. Swiech, G. Yang, and C. P. Flynn, Philos. Mag. Lett. **84**, 69 (2004); M. Ondrejcek, W. Swiech, M. Rajappan, and C. P. Flynn, Phys. Rev. B **72**, 085422 (2005).
- [28] N. C. Bartelt, T. L. Einstein, and E. D. Williams, Surf. Sci. Lett. **240**, L591 (1990).
- [29] T. J. Stasevich *et al.*, Phys. Rev. B **71**, 245414 (2005).
- [30] J. D. Shore and D. J. Bukman, Phys. Rev. Lett. **72**, 604 (1994); J. Neergaard and M. den Nijs, Phys. Rev. Lett. **74**, 730 (1995).
- [31] C. Tao, T. J. Stasevich, T. L. Einstein, and E. D. Williams, Phys. Rev. B **73**, 125436 (2006).